Journal of Cerebral Blood Flow & Metabolism (2013) 33, 600–611

www.jcbfm.com

ORIGINAL ARTICLE

$P2Y_1R$-initiated, IP_3R-dependent stimulation of astrocyte mitochondrial metabolism reduces and partially reverses ischemic neuronal damage in mouse

Wei Zheng[1], Lora Talley Watts[1], Deborah M Holstein[1], Jimmy Wewer[2] and James D Lechleiter[1]

Glia-based neuroprotection strategies are emerging as promising new avenues to treat brain damage. We previously reported that activation of the glial-specific purinergic receptor, $P2Y_1R$, reduces both astrocyte swelling and brain infarcts in a photothrombotic mouse model of stroke. These restorative effects were dependent on astrocyte mitochondrial metabolism. Here, we extend these findings and report that $P2Y_1R$ stimulation with the purinergic ligand 2-methylthioladenosine 5′ diphosphate (2MeSADP) reduces and partially reverses neuronal damage induced by photothrombosis. *In vivo* neuronal morphology was confocally imaged in transgenic mice expressing yellow fluorescent protein under the control of the Thy1 promoter. Astrocyte mitochondrial membrane potentials, monitored with the potential sensitive dye tetra-methyl rhodamine methyl ester, were depolarized after photothrombosis and subsequently repolarized when $P2Y_1Rs$ were stimulated. Mice deficient in the astrocyte-specific type 2 inositol 1,4,5 trisphosphate (IP_3) receptor exhibited aggravated ischemic dendritic damage after photothrombosis. Treatment of these mice with 2MeSADP did not invoke an intracellular Ca^{2+} response, did not repolarize astrocyte mitochondria, and did not reduce or partially reverse neuronal lesions induced by photothrombotic stroke. These results demonstrate that IP_3-Ca^{2+} signaling in astrocytes is not only critical for $P2Y_1R$-enhanced protection, but suggest that IP_3-Ca^{2+} signaling is also a key component of endogenous neuroprotection.

Journal of Cerebral Blood Flow & Metabolism (2013) **33,** 600–611; doi:10.1038/jcbfm.2012.214; published online 16 January 2013

Keywords: calcium signaling; dendritic damage; IP_3R type2 knockout; ischemic stroke; neuroprotection; purinergic receptor

INTRODUCTION

A cerebrovascular stroke is the rapid loss of brain function(s) due to disturbance in the blood supply to the brain. This can be due to ischemia caused by blockage or to a hemorrhage. Strategies to minimize brain damage and enhance neurological recovery after stroke have focused almost exclusively on neurons and resulted in minimal success. Recent evidence points to astrocytes as an alternative candidate for the development of novel stroke therapies.[1] Astrocytes are the most abundant cell type in the human brain and they are more resistant to ischemia than neighboring neurons. They naturally support neuronal survival and modulate neuronal recovery by providing metabolic and trophic support, glutamate and K^+ clearance, as well as antioxidant protection during ischemia.[2] In fact, the size of the ischemic infarct appears to be largely determined by the extent of astrocyte death.[2] Consequently, we have targeted astrocytes to enhance neuronal survival and minimize persistent brain damage after stroke.

At its core, cell death after stroke results from reduced oxygen and glucose, which decreases ATP production.[3] ATP depletion increases the influx of Na^+ ions into cells followed by Cl^- ions. This influx increases osmotic pressure and causes cell lysis if the blood supply is not rapidly restored. The most prominent astrocyte response to brain damage is cell swelling.[4] Na^+ influx also depolarizes cells, which stimulates an excessive release of the neurotransmitter glutamate in excitatory neurons causing excitotoxicity.[5] In general, excitotoxicity and cell lysis subsequent to osmotic expansion damage adjacent tissue and expand the infarct by secondary mechanisms.[2,6]

Although an ample supply of energy is fundamental to the ability of astrocytes to carry out their neuroprotective functions, it has only recently been demonstrated that astrocyte mitochondria play an important role in energy production.[7,8] Chu *et al*[9] reported that inhibition of glial mitochondria increases astrocyte swelling and leads to necrotic cell death. We reported a major protective role for astrocyte mitochondria subsequent to oxidative stress and stroke in mice.[10,11] We also reported $P2Y_1R$ stimulation decreased cytotoxic edema in astrocytes and lessened the size of brain infarcts.[11] In this manuscript, we extend these studies and show that $P2Y_1R$ stimulation of astrocyte mitochondrial metabolism also enhances neuronal survival and recovery after stroke. In addition, we establish the critical role of IP_3R-mediated Ca^{2+} signaling on this protective pathway. Given the pervasive energy demands of neuroprotective mechanisms, we propose that therapeutic strategies targeting astrocyte mitochondrial metabolism will be broadly applicable to multiple types of brain damage.

MATERIALS AND METHODS

Transgenic Animals and Surgical Procedures

Only male transgenic mice were used in our experiments given the significant influence of gender on stroke outcome in rodents. Adult (4 to 6 months) GFAP–green fluorescence protein (GFP) mice expressing GFP in astrocytes and Thy1–yellow fluorescent protein (YFP) mice (H-line) that

[1]Department of Cellular and Structural Biology, San Antonio, Texas, USA and [2]Institutional Optical Imaging Facility, University of Texas Health Science Center at San Antonio, San Antonio, Texas, USA. Correspondence: Professor JD Lechleiter, Department of Cellular and Structural Biology, University of Texas Health Science Center at San Antonio, 7703 Floyd Curl Drive, San Antonio, TX 78229-3900, USA.
E-mail: lechleiter@uthscsa.edu
This work was supported by grants from the National Institute of Health (AG29461 and AG19316).
Received 4 July 2012; revised 12 December 2012; accepted 13 December 2012; published online 16 January 2013

selectively expresses YFP in cortical layer 5 pyramidal neurons were obtained from The Jackson Laboratory (Bar Harbor, ME, USA) and bred at the University of Texas Health Science Center at San Antonio animal facilities. The IP_3R2 knockout mice were generated by Dr Ju Chen's group at the University of California-San Diego and obtained from Dr Ken McCarthy's laboratory at the University of North Carolina at Chapel Hill. Experimental procedures were identical to our previously published protocols.[11] Animal procedures were carried out in accordance with the Institutional Animal Care and Use Committee (IACUC) at University of Texas Health Science Center at San Antonio (Animal Welfare Assurance Number: A3345-01) and with the ARRIVE guidelines.[12] Mice were anesthetized with isofluorane and their body temperature was maintained at 37 °C by a heating pad (Gaymar T/Pump). Their scalp was shaved and incised in the midline. Then the skull was exposed, cleaned and glued (VetBond, 3M, St Paul, MN, USA) to a stainless steel ring attached to a custom-made stereotaxic frame. A small portion of the skull overlying the somotosensory cortex (between ~1 to ~3 mm postbregma and 2 to 4 mm lateral) was initially thinned by variable-speed electric drill (Fine Science Tools, Foster City, CA, USA) and further thinned to ~50 μm by a surgical blade to either create a thin-skull cranial window or an open-skull cranial window by removing the skull using a fine-tipped forceps (0.01 mm, Dumont, Fine Science Tools). To achieve an open-skull window, subsequent manual removal of the dura with a fine-tipped forceps was carefully performed under aCSF (artificial cerebrospinal fluid) containing 126 mM NaCl, 2.5 mM KCl, 1.25 mM NaH_2PO_4, 2 mM $MgCl_2$, 2 mM $CaCl_2$, 10 mM glucose, and 26 mM $NaHCO_3$ (pH 7.4). Then the cortical surface was washed and the cranium hole sealed by filling it with 2% agarose (type VII, low gelling temperature, Sigma, St Louis, MO, USA). A glass coverslip (#0) was then pressed against the skull to allow optimal imaging with a high numerical objective (60 × LUMFL NA 1.1 with correction collar, Olympus, Tokyo, Japan).

Stroke Induction by Rose Bengal Photothrombosis and Drug Administration

Photochemical reaction of Rose Bengal activates tissue factor, the initiator of the coagulation cascade, and consequently triggers the extrinsic coagulation cascade, therefore producing an ischemic lesion that is pathologically very relevant to clinical stroke. Focal cerebral ischemic stroke was induced by photochemical thrombosis as previously described.[11] In brief, 10 mg/mL sterilized Rose Bengal dissolved in PBS (phosphate-buffered saline) (Sigma) was tail-vein injected. Photothrombosis was performed by exposing a targeted cortical arteriole (20 to 30 μm) to green light (543 nm, 5 mW) through a 0.8-NA 40 × water-immersion objective (Nikon, Tokyo, Japan). Stable clot formation was confirmed by occlusion of downstream capillaries. According to our previous studies, the blood–brain barrier breaks down within 10 minutes of an RB-induced ischemic stroke and remains disrupted for at least 2 days following photothrombosis.[11] Loss of the blood–brain barrier allowed us to introduce pharmacological reagents at the same time a stroke was induced. $P2Y_1R$-specific agonists 2MeSADP (0.25 mg/kg, 100 μM) was administrated by tail-vein injection.

Neuronal Dendrite Imaging, Astrocyte Ca^{2+} and $\Delta\psi$ Imaging

In vivo imaging was performed as previously described[11] by utilizing an Olympus FV1000 MPE with a 10 × 0.45 NA dry, 40 × 0.8 NA or 60 × 1.1 NA water objective. For neuronal dendritic imaging, high-resolution *z* stacks of layer one cortical dendrites containing a clotted vessel were acquired before and after RB-induced, ischemic stroke. Dendritic beading was quantified following the procedures outlined by Dr Murphy's group.[13,14] In brief, maximal intensity projections of cortical *Z* stacks were performed preclot, postclot and post-2MeSADP to obtain two-dimensional (D) images under each condition. These 2D images were registered and aligned using stackreg of NIH Image J software (National Institutes of Health, Bethesda, MD, USA) to facilitate identification and comparison of same dendrites. The preclot image was utilized as a reference and colored green. The images of postclot and post-2MeSADP cortex were colored red and merged with the green preclot image. The merged green − red images were utilized to count beading percentage manually using Grid and Cell counter plugins of image J. A grid of 20 × 20 μm^2 blocks was overlaid on a merged green − red image for analysis. Blocks with blebbed dendrites were identified, counted and reported as a beading percentage utilizing Cell counter. We note that blebbed dendrites were larger in diameter than their corresponding reference dendrites and exhibited a typical 'string of beads' appearance as previously reported.[13,14] For calcium imaging, the exposed mouse cortex was incubated with cytosolic Ca^{2+} indicator dye Fluo4-AM. Fluo4-AM was dissolved in 5 μL DMSO mixed with 2 μL of Pluronic and diluted in 30 μL artificial cerebral spinal fluid (aCSF). Following 1-hour incubation, the excess dye was washed off by aCSF. The cortical loading of Fluo4-AM is highly specific for astrocyte labeling *in vivo*.[15] For mitochondrial membrane potential imaging, potential sensitive dye tetramethyl rhodamine methyl ester (TMRM) was dissolved in DMSO, diluted in sterilized PBS (100 μM) and tail-vein injected. Tetra-methyl rhodamine methyl ester is a lipophilic cation indicator that equilibrates across membranes in a Nernstian fashion. It accumulates in the mitochondrial matrix in inverse proportion to the mitochondrial membrane potential.[16] Consequently, tail-vein injections of TMRM permeate the blood–brain barrier and label brain mitochondria. Presumably because of their proximity to blood vessels, our data indicate that tail-vein loading of TMRM preferentially labels astrocyte mitochondria. We demonstrated that TMRM-stained peri-nuclear mitochondria colocalize with cells that can be labeled with the astrocyte-specific dye sulforhodamine 101 (SR101)[15] as shown in Figures 4D and 4F. To correct for spectral overlap in Figures 4D and 4F, the TMRM image at 6 hours was subtracted from the SR101 plus TMRM image at 7 hours after RB photothrombosis. This correction procedure assumes minimal movement of TMRM-labeled mitochondria during the 1-hour labeling period with SR101 dye. We checked and confirmed the lack of significant movement by observing essentially no TMRM fluorescent signal outside of SR101-labeled astrocytes in the final corrected image. We noted that astrocytes can be identified in the absence of SR101 staining because of their large-round nuclei (Figure 3). This observation is consistent with images being acquired in layer 1 of the cortex, where very few neuronal nuclei exist and the size of microglia nuclei are significantly smaller.[17] Consequently, their size and abundance make astrocyte nuclei very distinctive. This approach showed no significant influence on neuronal dendrite and astrocyte morphology (Figure 3). Cortical application of 100 μM FCCP significantly decreased TMRM fluorescence with 30 seconds (Figure 3C), suggesting a nonquench staining pattern of TMRM. We initially assigned single mitochondria to specific astrocytes by using GFAP–GFP transgenic mice and subsequently found that bright circular nuclei of GFP-labeled astrocytes were completely colocalized with large, dark, rounded nuclei of Hoechst loaded cells (Figures 3A and 3B). This typical staining pattern of TMRM in cortical astrocytes was utilized to identify astrocytes and their mitochondria in Thy1–YFP mice. The virtual absence of significant movement of mitochondria *in vivo* enabled real-time measurements of $\Delta\psi$. Estimates of $\Delta\psi$ were made as previously described.[10] $\Delta\psi$ is expressed as the $(-60\text{ mV})\log(\text{Fmito/Fcyto})$, where Fmito is the peak fluorescent intensity observed in single mitochondria and Fcyto represents the lowest value of TMRM fluorescence observed over nuclei. The confocal excitation and emission spectra for fluorescent dyes are as following: TMRM was excited at 543 nm, and emission was collected through a 565 to 615 nm barrier filter. YFP was excited using a 514-nm argon laser line and the emission was collected between 535 to 580 nm. Fluo4-AM was excited at 488 nm and emission was collected through a 500 to 540 nm barrier filter. Hoechst 33342 was excited at 405 nm and emission was collected through a 420 to 460 nm. SR101 was excited with a HeNe green laser (543 nm) and detected in the 590 to 680 nm range.

Neuronal Lesions Evaluation Following Photothrombotic Stroke

As previously described,[11] *in vivo* assessment of ischemic neuronal lesions was performed by measuring the infarction border identified by the absence of YFP fluorescence and the absence of 2,3,5-triphenyltetrazolium chloride (TTC) staining. Multiple overlapping *Z*-stacks with 2 μm stepsize were taken from nearby region of clotted vessel 24 hours postthrombosis on Thy1–YFP transgenic mice, IP_3R2 KO-Thy1–YFP mice and littermate controls. Mosaic reconstruction of maximum intensity projections of overlapping image stacks was performed by using MosaicJ plug-in of NIH imageJ software to determine the infarction border.

Statistical Analyses

One-way analysis of variance was used to compare the differences among three or more groups. *t*-Test was used to compare the difference between two groups. The significance level is set at $P<0.05$. Data are presented as mean ± standard error (s.e.) of the mean. Prism software (Graphpad, La Jolla, CA, USA) was used to perform statistical analyses.

RESULTS

$P2Y_1R$ Stimulation Reduces RB-Induced Ischemic Neuronal Lesions in Mouse

As previously reported, we significantly reduced the size of cerebral infarcts induced by photothrombosis by stimulating

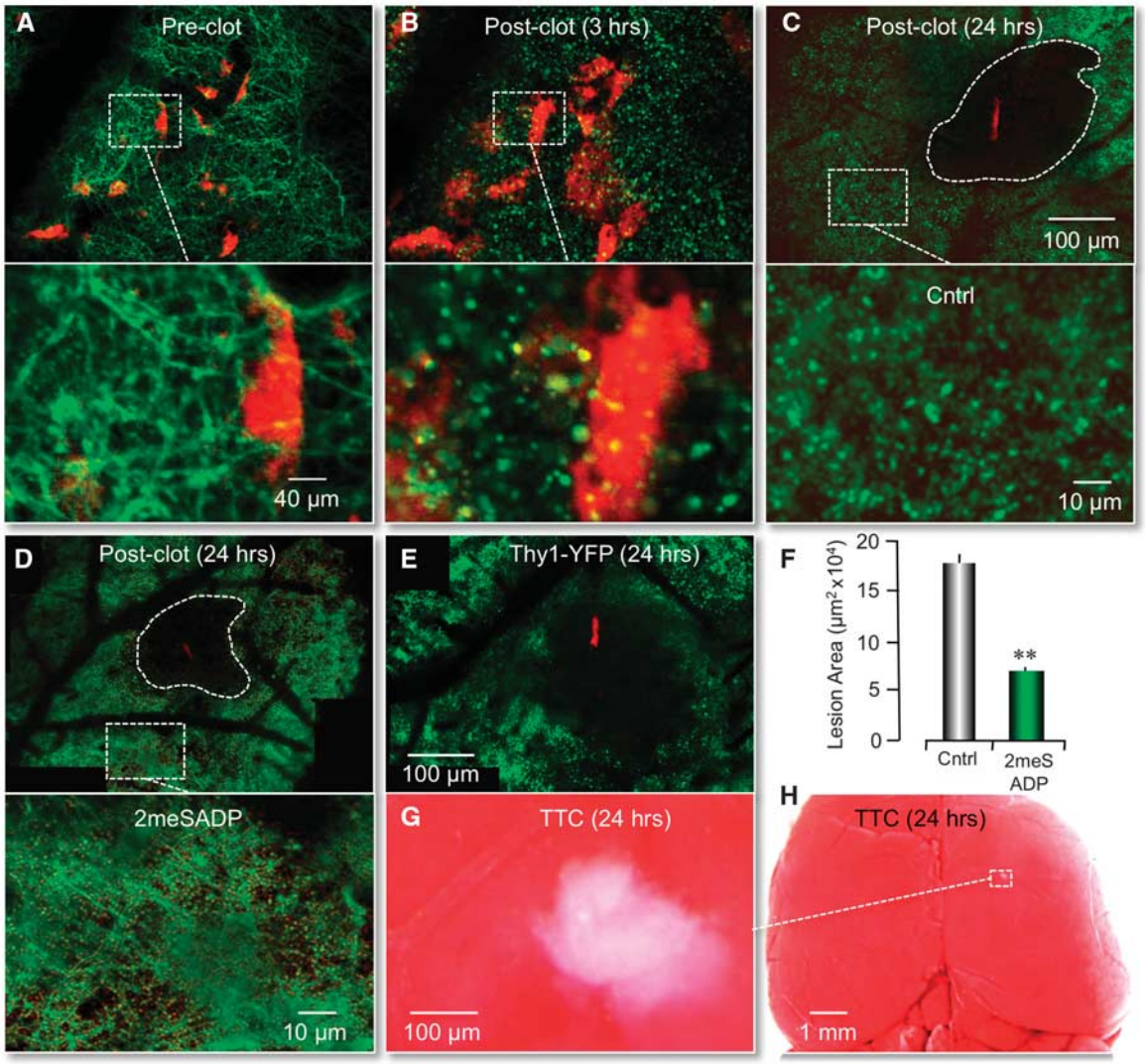

Figure 1. RB-induced neuronal lesions reduced by 2MeSADP treatment. (**A**, **B**) Fluorescent images in a mouse cortex showing a dendritic network (green pixels) and single astrocytes (red pixels) before and 3 hours after an RB-induced photothrombosis. The transgenic mice expressed yellow fluorescent protein (YFP) in neurons (Thy1–YFP) and green fluorescent protein (GFP) in astrocytes (GFAP–GFP). The primary clot is off the field of view. Note the significant neuronal dendrite beading and astrocyte swelling 3 hours post-RB photothrombosis. (**C**, **D**) Mosaic reconstruction of the parietal cortex of live Thy1–YFP mice 24 hours after RB-induced photothrombosis. Cerebral infarcts were evaluated by the absence of YFP fluorescence. The clot is identified by the red fluorescence of trapped RB dye. Note a significant reduction of lesion size after 2MeSADP treatment. White dashed rectangles correspond to higher magnification images of cortical areas near infarcts, indicating less neuronal dendrite beading with 2MeSADP treatment. (**F**) Histogram plot of the average neuronal lesion size of four control mice (RB only) and four experimental mice (RB + 2MeSADP) 24 hours postphotothrombosis. $^{**}P < 0.001$. (**E**, **G**, **H**) A single-vessel RB-induced ischemic lesion 24 hours postphotothrombosis is defined by both Thy1–YFP fluorescence and TTC staining. Note that the absence of YFP fluorescence in (**E**) is comparable to the absence of TTC staining in (**G**). A lower magnification of the TTC-defined lesion is identified in (**H**) by the white dashed rectangle.

astrocyte-specific $P2Y_1$Rs with the purinergic ligand 2-methylthioladenosine 5′ diphosphate (2MeSADP).[11] These studies were performed in transgenic mice expressing GFP in astrocytes, which permitted us to define the size of a lesion as the absence of GFP fluorescence (cell lysis). TTC staining of cortical infarcts was also performed in these previous studies to confirm loss of GFAP–GFP fluorescence accurately defined lesions following RB photothrombosis. Here, we wanted to determine how $P2Y_1$R stimulation affected neuronal viability after ischemic damage. To accomplish this, we optically imaged layer one of the cerebral cortex of transgenic mice expressing YFP in neurons (Thy1–YFPH) using previously described protocols.[11] When single-vessel ischemic clots were induced by irradiation of tail-vein-injected Rose Bengal (RB), we observed swelling and beading of dendritic structure in the absence of neuronal death (Figures 1A and 1B). These morphological changes are an early hallmark of ischemic neuronal injury as initially reported by Li and Murphy in 2008. Twenty-four hours after the photothrombosis, neuronal cell death, that is cell lysis, was apparent and an infarction border could easily be identified by the absence of YFP-labeled dendrites near the clotted blood vessel (Figure 1C). Again, we confirmed the validity of defining lesions as the absence of YFP fluorescence by TTC staining (Figures 1E, 1G, and 1H) and costaining with a nuclear DNA stain, Hoechst (Supplementary Figure 1). The extent of neuronal loss, $18.1 \pm 0.8\,\mu m^2 \times 10^4$ ($n = 4$) at 24 hours was significantly larger than the lesion defined by astrocyte death $10.2 \pm 0.7\,\mu m^2 \times 10^4$ ($n = 5$). These data were consistent with previous studies in cell culture, as well as those of others,[18] indicating cortical astrocytes were more resistant to ischemia than neurons *in vivo* (Supplementary Figure 2). To test the impact of

$P2Y_1R$ stimulation on neuronal viability, we coinjected another cohort of mice with 2MeSADP. As we observed for lesions defined by astrocyte cell lysis, we found that the size of neuronal lesions was significantly reduced to $7.9 \pm 0.4\ \mu m^2 \times 10^4$ ($n = 4$, $P < 0.001$) at 24 hours (Figures 1D and 1F).

$P2Y_1R$ Stimulation Partially Reverses RB-Induced Ischemic Neuronal Dendritic Damage

Swelling and beading of dendrites does not necessarily represent irreversible damage to neurons.[19] Normal morphology can be rescued by early restoration of blood flow after ischemia.[13] In contrast, if left unchecked, progression of dendrite beading and swelling leads to dendritic loss and neuronal cell death. A key requirement for recovery appears to be an adequate energy supply.[19] Consequently, we tested whether $P2Y_1R$ stimulation could reverse ischemic dendritic injury. A single-vessel clot was induced with photothromobisis, then dendritic swelling and beading were permitted to develop. Three hours after the initial photothrombosis, 2MeSADP was tail-vein injected into the ischemic mouse. We observed significant reversal of dendritic beading and swelling within 1 hour of 2MeSADP treatment, which continued for at least another 2 hours (Figures 2A–2C). The percentage of dendrites exhibiting beading decreased to $88.7\% \pm 3.6\%$ at 1 hour, $77.2\% \pm 6.1\%$ at 2 hours, and $62.6\% \pm 6.1\%$ at 3 hours posttreatment ($n = 4$), compared with control values of $97.0\% \pm 5.1\%$, $97.2\% \pm 5.2\%$, and $98.1\% \pm 6.8\%$ ($n = 4$), respectively (Figures 2D–2G). Thus, 2MeSDP treatment in the absence of reperfusion at least partially reversed ischemic dendritic damage. Consistent with previous reports,[13] we note that neither laser illumination nor the RB dye by itself affected dendrite beading (data not shown).

$P2Y_1R$-Enhanced Neuroprotection Correlates with Reversal of RB-Induced Mitochondrial Depolarization in Astrocytes

Our previous studies indicated that $P2Y_1R$-mediated neuroprotection depends on astrocyte mitochondrial metabolism.[11,20] This mechanism predicts that ischemia-induced changes in dendritic morphology correlate with changes in astrocyte mitochondrial potentials. To test this prediction, Thy1–YFP mice were prepared for *in vivo* imaging as previously described and then tail-vein injected with the potential sensitive dye TMRM (0.1 mL of 100 μM TMRM). This procedure rapidly labels all mitochondria within minutes, with TMRM fluorescence remaining stable for at least 3 hours (Figures 3D–3H). Subcellular images of individual mitochondria in the proximity of YFP-labeled neuronal dendrites were recorded using this technique (Figure 4A). A subpopulation of mitochondria near morphologically distinct nuclei was attributed to astrocytes based on the observations that neuronal nuclei are generally absent in layer one of the cortex and that microglial nuclei are significantly smaller than astrocyte nuclei labeled with GFP or SR101 (Figures 3A and 3B and 4F). When a single vessel, RB-induced photothrombosis was induced, we observed significant mitochondrial depolarization in parallel with dendritic beading and swelling (Figures 4B, 4G–4I). The mean mitochondrial potential decreased from -146.8 ± 6.0 ($n = 3$) in control cells to -122.3 ± 6.3 ($n = 3$) 3 hours after photothrombosis (Figure 4J). When the $P2Y_1R$ ligand, 2MeSADP, was tail-vein injected at 3 hours postclot, we observed a significant repolarization of astrocyte mitochondria to -148.3 ± 5.0 ($n = 3$), as well as a partial reversal of the neuronal beading and swelling (Figures 4C and 4E). A control mouse in which saline was tail-vein injected at 3 hours postclot exhibited continued mitochondrial depolarization and dendritic damage (Figures 4G–4I).

IP_3-Mediated Ca^{2+} Release Is Required for $P2Y_1R$-Mediated Reversal of RB-Induced Mitochondrial Depolarization in Astrocytes

We demonstrated that $P2Y_1R$-enhanced neuroprotection can be pharmacologically blocked by treating astrocytes with the mitochondrial Ca^{2+} uniporter inhibitor, ruthenium360, with the ATP synthesis inhibitor, oligomycin, as well as with the tricarboxylic acid cycle inhibitor, fluoroacetate.[11,20] We have also reported that $P2Y_1R$-enhanced neuroprotection can be genetically blocked by expression of a mitochondrially targeted DNA restriction enzyme, mtEcoR1, which specifically disrupts astrocyte mitochondrial function.[11] Here, we directly tested whether the $P2Y_1R$-enhanced mitochondrial metabolism was dependent on the inositol 1,4,5 trisphosphate receptor (IP_3R). IP_3R type2 knockout mice were utilized, since their astrocytes lack spontaneous and G-protein coupled receptor mediated Ca^{2+} increases.[21] IP_3R type2 knockout or control wild-type mice were prepared for *in vivo* cortical imaging using an open-skull preparation, which permitted cortical loading of the Ca^{2+} indicator dye Fluo-4 AM.[22] Mice were then treated and imaged as described above, including tail-vein injection of rose Bengal (RB) and 2MeSADP (100 μM). We found that after an RB-induced photothrombosis, leakage of 2MeSADP across the blood–brain barrier elicited Ca^{2+} increases in astrocytes in control wild-type mice (Figures 5A and 5B), but not in IP_3R type2 knockout mice (Figures 5C and 5D), consistent with the observations of Petravicz and coworkers.[21] The average peak amplitude of wild-type astrocytic Ca^{2+} responses within 50 μm of the clotted vessel was 0.76 ± 0.09 ($\Delta F/F$, $n = 3$ mice pooled from 51 cells). Direct measurements of the blood vessel diameter, before (32.3 ± 4.2, $n = 6$) and after (31.8 ± 5.1, $n = 7$) astrocytic Ca^{2+} revealed no acute changes in the vasculature. Next, we crossed IP_3R type2 knockout mice with Thy1–YFP mice to enable *in vivo* imaging of neuronal morphology and then tail-vein injected the potential sensitive dye TMRM to determine the impact of IP_3R type2 activity on mitochondrial membrane potentials. We found no significant differences in astrocyte mitochondrial membrane potentials under basal conditions, with and without IP_3Rs type2. In contrast, after we challenged these mice with an RB-induced ischemic stroke, the mitochondrial membrane potential in astrocytes from IP_3R type2 knockout mice was found to be significantly lower than littermate controls 3 hours postphotothrombosis. The average potential was (-107.6 ± 6.3 mV, $n = 3$) in IP_3R type2 astrocytes and (-122.3 ± 6.3 mV, $n = 3$) in wild-type, control mice (Figures 6E–6H cf. Figures 4G–4J, data pooled from three mice). Moreover, administration of 2MeSADP, 3 hours after the initial photothrombosis, failed to reverse the RB-induced mitochondrial depolarization in astrocytes in IP_3R type2 knockout mice (Figures 6A–6D). These experiments indicate that IP_3-Ca^{2+} signaling plays a critical role not only in mediating $P2Y_1R$-enhanced mitochondrial metabolism, but also in enhancing mitochondrial metabolism postischemia in the absence of 2MeSADP.

Astrocyte IP_3-Mediated Ca^{2+} Release Is Required for $P2Y_1R$-Mediated Decreases in RB-Induced Ischemic Neuronal Lesions and Dendritic Damage

Finally, we wanted to directly test whether the $P2Y_1R$-enhanced neuroprotective pathway was dependent on the IP_3R type2. We again utilized the IP_3R2 knockout x Thy–YFP mice and measured the effect of RB-induced ischemic lesions. First, we found that the average size of RB-induced ischemic lesions in IP_3R type2 knockout mice, even in the absence of $P2Y_1R$ stimulation, was significantly increased to $52.7 \pm 4.9\ \mu m^2 \times 10^4$ ($n = 4$) This represented a $195.2\% \pm 16.1\%$ increase compared with littermate wild-type controls at 24 hours postphotothrombosis (Figure 7A, cf. Figure 1C). Second, we found no evidence that the average size of RB-induced neuronal lesions at $57.6 \pm 4.2\ \mu m^2 \times 10^4$ ($n = 4$) was changed at 24 hours, when mice were tail-vein injected with 2MeSADP (Figures 7B and 7C). Third, we determined that delayed treatment of mice with 2MeSADP, 3 hours after the initial RB-induced photothrombosis, failed to reduce or partially reverse the neuronal dendritic beading and swelling (Figures 7D–7H).

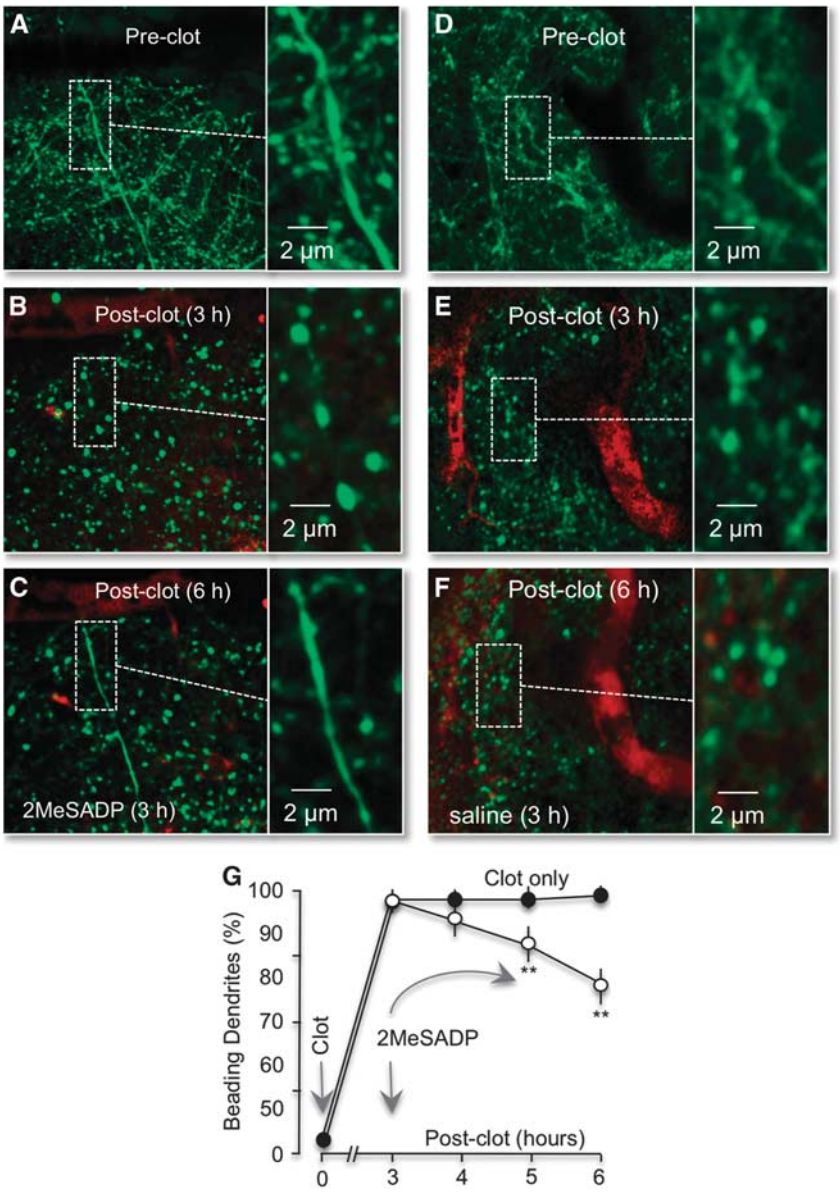

Figure 2. $P2Y_1R$ stimulation by 2MeSADP reverses neurite damage following photothrombosis. (**A**–**C**) Confocal images from a Thy1–YFP mouse (dendrites colored green) after an RB-induced clot (red) before, 3 and 6 hours after photothrombosis. Images are maximal intensity *Z* projections of $\sim 70\,\mu$m of layer one cortical dendrites containing the clotted vessel. 2MeSADP (100 μM) was administrated by tail-vein 3 hours postphotothrombosis. Regions marked by white dashed rectangles are enlarged on the right. Note the ischemic neuronal beading 3 hours after photothrombosis and the reversal of beading 3 hours post-2MeSADP treatment. (**D**–**F**) Delayed saline does not reverse RB-induced dendritic damage. Confocal images of acute ischemic neuronal dendritic beading (green) induced by RB photothrombosis in a Thy1–YFP mice shown before photothrombosis (**D**) and 3 (**E**) and 6 (**F**) hours postphotothrombosis. Saline was injected 3 hours postthrombosis. Clotted blood vessels are colored red. (**G**) Line plot of the number of dendrites with beading at 3, 4, 5, and 6 hours postthrombosis with and without 2MeSADP treatment ($n = 4$). $^{**}P < 0.01$.

We concluded that $P2Y_1R$-enhanced neuroprotection and partial reversal of dendritic damage is dependent on expression of the IP_3R type2 in astrocytes.

DISCUSSION

Astrocyte-mediated neuroprotection after brain damage is gaining wide acceptance.[1] We previously reported that neuroprotection could be enhanced by stimulating astrocyte-specific $P2Y_1Rs$. This enhanced protection could be blocked by inhibitors of mitochondrial Ca^{2+} uptake (Ru360) and ATPsynthase activity (oligomycin).[20] Measurements showed that $P2Y_1R$ stimulation, as well as direct addition of membrane permeable IP_3 to astrocytes, increased mitochondrial O_2 consumption and ATP production.[20] The *in vivo* neuroprotective effects appeared to act by increasing mitochondrial metabolism and not by affecting vasodilation, clot stability or microglia.[11] Our working model assumes that stimulation of $P2Y_1Rs$ generates IP_3, which binds to the IP_3R, releasing Ca^{2+} from the endoplasmic reticulum. We further assume that Ca^{2+} is sequestered by mitochondria, ultimately leading to increased ATP production by increasing the membrane potential via stimulation of Ca^{2+}-sensitive dehydrogenases in the tricarboxylic acid cycle and the ATPsynthase. Ca^{2+}-stimulated production of ATP was initially characterized in cardiac muscle mitochondria, which increased energy production up to 10-fold faster than stimulation by ADP.[23] Here, we tested and extended

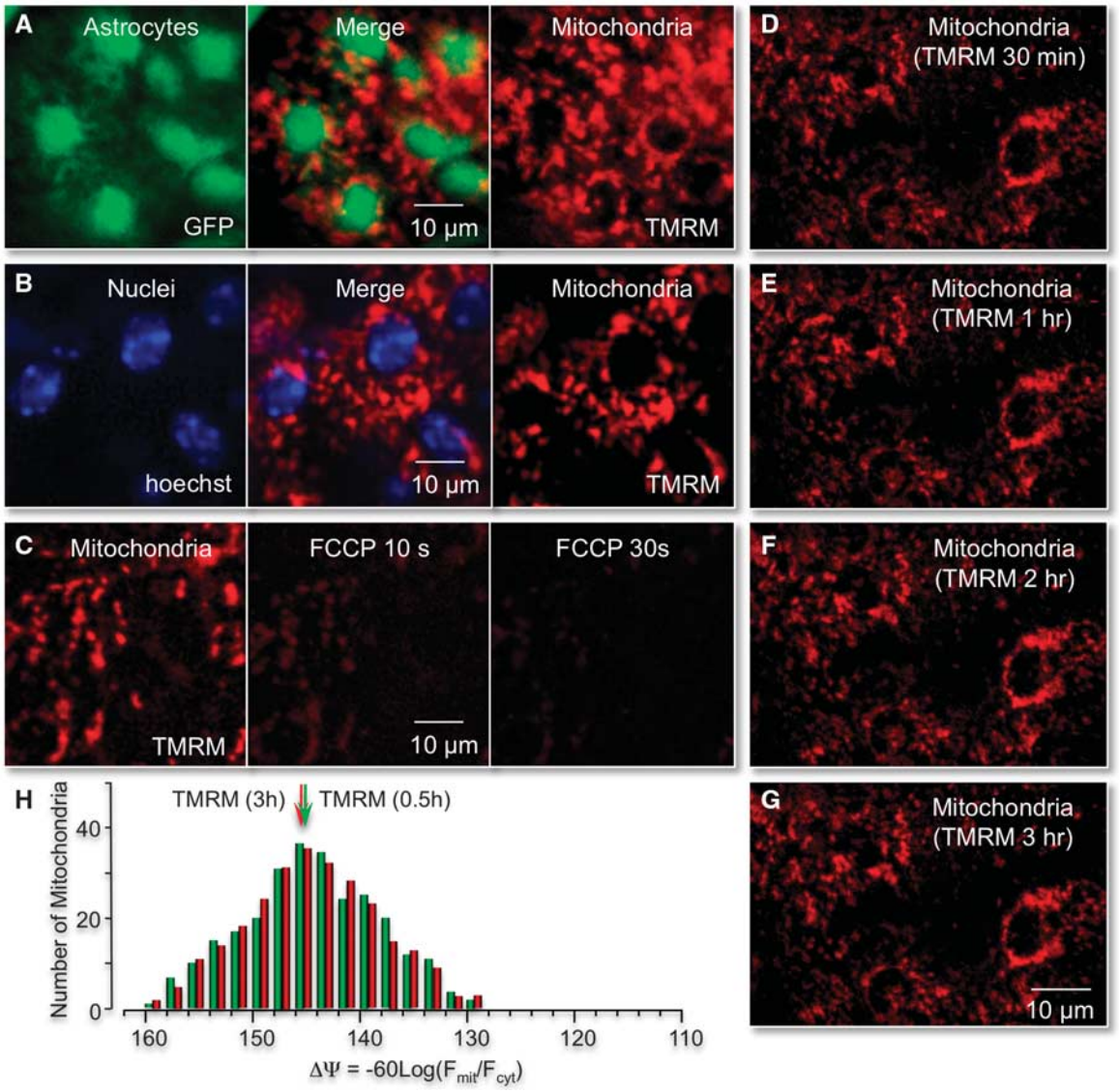

Figure 3. Identification of astrocyte mitochondria *in vivo*. (**A**) Cortical image of a transgenic mice expressing green fluorescent protein (GFP) in astrocytes (GFAP–GFP) and tail-vein injected with tetra-methyl rhodamine methyl ester (TMRM). (**B**) Same cortical region shown in (**A**), but imaged after tail-vein injection of the nuclear stain hoechst 33342. Note large, rounded soma of astrocytes (labeled green) colocalizes with nuclei (labeled blue). Individual mitochondria surrounding large-round nuclei were assigned to specific astrocytes. Images were obtained by maximal intensity *Z* projections of $\sim$40 μm cortical layer I. (**C**) Cortical application of the *mitochondrial uncoupler* FCCP (100 μM) significantly decreased TMRM fluorescence within 30 seconds, demonstrating functional TMRM labeling of polarized mitochondria. (**D**–**G**) Fluorescent labeling of cortical mitochondria with tail-vein injections of TMRM is stable for at least 3 hours. Maximal intensity image projections of *Z* stacks of mitochondria in layer one of the mouse cortex 30 minutes, 1, 2, and 3 hours after tail-vein injection of TMRM. (**H**) Histogram plot of the distribution of individual mitochondrial potentials ($\Delta\Psi$) 30 minutes and 3 hours post-TMRM injection.

Figure 4. $P2Y_1R$ stimulation with 2MeSADP reverses astrocytic mitochondrial depolarization induced by photothrombosis. (**A**–**D**) *In vivo* confocal images of neuronal processes from Thy1–YFP transgenic mice (green pixels), which were tail-vein injected with the mitochondria dye tetra-methyl rhodamine methyl ester (TMRM) before RB photothrombosis (**A**), 3 hours after photothrombosis (**B**), 6 hours after photothrombosis (**C**) and cortically loaded with astrocyte-specific dye sulforhodamine 101 (SR101) 3 hours after 2MeSADP treatment (**D**). The RB-induced clot is identified at the upper right-hand corner of each panel with the open arrow head. The $P2Y_1R$ ligand 2MeSADP (100 μM) was administrated 3 hours postphotothrombosis (**B**). Regions marked by white dashed rectangles are presented at higher magnification below each panel. Note the significant mitochondrial depolarization in parallel with dendritic beading 3 hours postthrombosis. Tail-vein injection of 2MeSADP at 3 hours postclot repolarizes astrocyte mitochondria and partially reverses neuronal beading (**C**). The astrocyte-specific dye, SR101 (100 μM), was then cortically loaded for 60 minutes, 3 hours after 2MeSADP treatment (**D**). Note that SR101 labels cells with large-round nuclei, as indicated in Figure 3. (**F**) Colocalization of SR101-labeled astrocytes (red) with TMRM-stained mitochondria (green) prephotothrombosis. Note mitochondria near large-round nuclei are contained within SR101 staining. (**E**) Histogram plot of the distribution of membrane potentials ($\Delta\Psi$) from mitochondria near astrocyte nuclei with 2MeSADP treatment before, 3 and 6 hours after photothrombosis. (**G**–**J**) Administration of saline 3 hours postphotothrombosis does not repolarize astrocyte mitochondria or reverse dendrite beading. *In vivo* confocal images of neuronal processes from Thy1–YFP transgenic mice (green pixels) plus astrocyte mitochondria labeled with TMRM before RB photothrombosis (**G**), 3 (**H**) and 6 hours after photothrombosis (**I**). (**J**) Histogram plot of the distribution of membrane potentials ($\Delta\Psi$) from mitochondria near astrocyte nuclei with saline treatment before, 3 and 6 hours after photothrombosis.

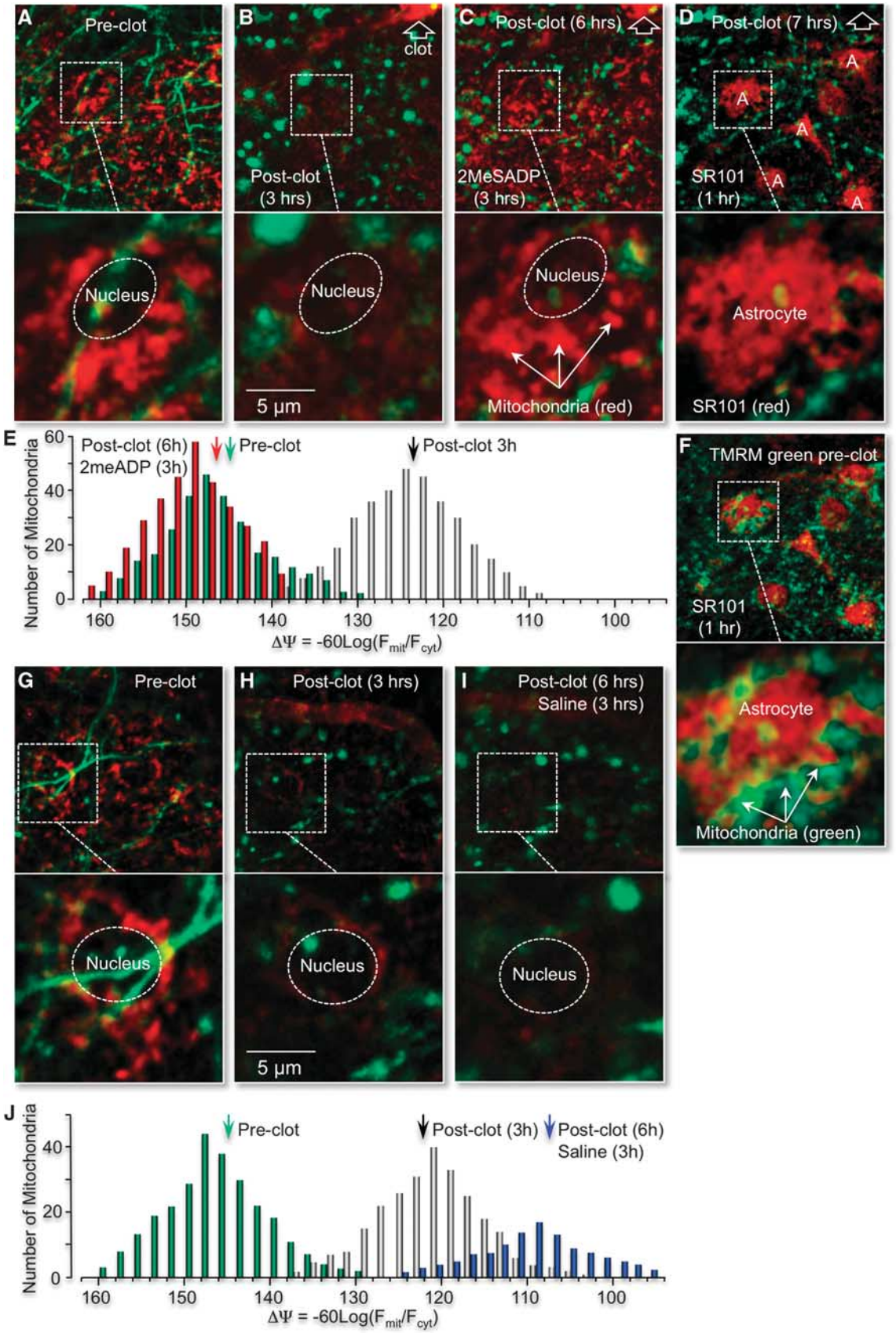

Figure 4. For caption refer page 605.

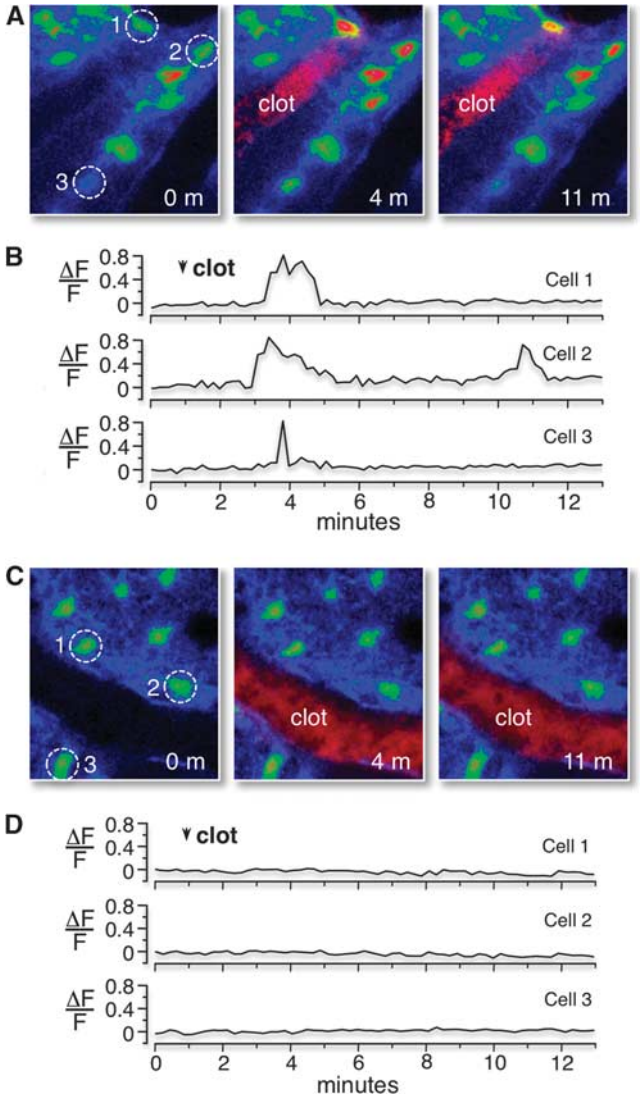

Figure 5. Tail-vein injection of 2MeSADP induces Ca^{2+} increases in wild-type control astrocytes after photothrombosis, but not in astrocytes of IP_3R2 KO mice. (**A**) Confocal images of the Ca^{2+} responses in wild-type control mice loaded with the Ca^{2+} indicator fluo4-AM before RB-induced photothrombosis, and 3 and 10 minutes after RB photothrombosis. Clotted vessel appears in the middle panel (red pixels with label). Ca^{2+} levels (fluo4 fluorescence) are color-coded (blue is lowest concentration, red is highest concentration). The $Ca2^{+}$ levels of three cells (identified by dashed circles) are followed before and after 2MeSADP leakage across the blood–brain barrier. (**B**) Single-line traces of the Ca^{2+} responses from these three cells are plotted ($\Delta F/F$). (**C**) Confocal images of Ca^{2+} response in IP_3R2 KO mice before, and 3 and 10 minutes after RB photothrombosis. Imaging and presentation identical to wild-type mice. (**D**) Single-line traces of representative Ca^{2+} response of the cells identified in image panels.

our model in four important ways. We directly demonstrated that $P2Y_1R$ stimulation of astrocytes reduced neuronal damage and cell death. We determined that ischemia-induced brain damage and swelling were partially reversed by $P2Y_1R$ stimulation. We established that enhanced neuroprotection correlated with increased mitochondrial metabolism in astrocytes. Finally, we demonstrated that all of these $P2Y_1R$-stimulated actions depended on astrocyte-specific IP_3R expression.

IP_3-mediated Ca^{2+} release in astrocytes has long been recognized as a major component of the early ischemic response.[24] However, the functional implications of Ca^{2+} following ischemia have not been resolved, with both protective and detrimental effects identified. Several groups reported that IP_3-Ca^{2+} signaling counteracted the development of ischemic brain edema via its role in regulatory volume decrease.[25] These data are consistent with the findings we presented here and previously.[11] On the other hand, Ding *et al*[26] demonstrated that astrocyte Ca^{2+} signaling increased excitotoxic neuronal injury following ischemia, possibly via the Ca^{2+}-dependent release of glial glutamate. Their data and ours are not necessarily contradictory and may simply reflect multiple Ca^{2+} targets within astrocytes as well as differential Ca^{2+} responses related to either receptor subtype or the location and duration of a Ca^{2+} response. For example, Shigetomi *et al*[27] found stimulation of both $P2Y_1Rs$ and proteinase-activated receptors (PAR-1s) increased intracellular Ca^{2+} in astrocytes, but only activation of PAR-1s resulted in significant release of glutamate from astrocytes and neuronal toxicity. Shigetomi *et al*[27] suggested that this was related to the modes of glutamate exocytosis triggered by these agonists, the spatial location of the glutamate release sites or the duration of the Ca^{2+} transients. The time scale and magnitude of the Ca^{2+} response may also be critical. Photothrombotic ischemia can induce significant Ca^{2+} increases in astrocytes but this generally takes much longer than the time frame we observe $P2Y_1R$-induced changes (Figures 5A and 5B). Specifically, Ding *et al*[26] showed that it takes ~30 to 40 minutes to observe significant increases in somatic Ca^{2+} increases after a large photothrombosis. In contrast, our $P2Y_1R$ ligand 2MeSADP, introduced via tail injection, increased astrocyte Ca^{2+} within 10 minutes.

The studies presented here have further defined the neuroprotective role of astrocyte IP_3-Ca^{2+} signaling in the ischemic brain by utilizing a mouse model deficient in the only IP_3R isoform expressed in astrocytes, the IP_3R2.[21] These knockout mice exhibit no significant changes in Ca^{2+}-dependent gliotransmitter release under normal conditions and there do not appear to be any histological or behavioral abnormalities.[21] We found the size of ischemic lesions was not reduced by $P2Y_1R$ stimulation in IP_3R2 knockout mice and delayed treatment of these mice with the $P2Y_1R$ ligand 2MeSADP did not reverse dendritic damage. We concluded that $P2Y_1R$-enhanced neuroprotection was dependent on IP_3R2 signaling. It should be noted, however, that the size of photothrombotic-induced ischemic lesions was increased in the absence of the IP_3R2 isoform, even in the absence of $P2Y_1R$ stimulation (Figure 7). This observation is comparable to the data we previously reported showing disruption of mitochondrial function in astrocytes, either pharmacologically or genetically, resulted in larger ischemic lesions in the absence of $P2Y_1R$

Figure 6. $P2Y_1R$ stimulation with 2MeSADP does not reverse RB-induced mitochondrial depolarization in astrocytes or dendritic damage in neurons of IP3R2 knockout ($-/-$) mice. (**A**–**C**) *In vivo* confocal images of mitochondria (red pixels, tetra-methyl rhodamine methyl ester (TMRM)) and neuronal process from $IP_3R2-/-$ mice (green) before (**A**), 3 (**B**) and 6 hours after photothrombosis (**C**). Image acquisition and presentations are identical to Figures 4A–4C. (**D**) Histogram plots of astrocyte mitochondrial potential distributions for the IP_3R2 KO mice before and after photothrombosis, with 2MeSADP treatment as indicated. (**E**–**G**) Administration of saline 3 hours postphotothrombosis does not repolarize astrocyte mitochondria or reverse dendrite beading in IP3R knockout ($-/-$) mice. Confocal images dendrites (green pixels) and astrocyte mitochondria (red pixels) before RB photothrombosis (**E**), and 3 (**F**) and 6 hours after photothrombosis (**G**). Imaging protocols and presentations are identical to those presented in Figures 4E–4G. (**H**) Histogram plots of astrocyte mitochondrial potential distributions for the IP_3R2 KO mice before and after photothrombosis, with saline treatment as indicated.

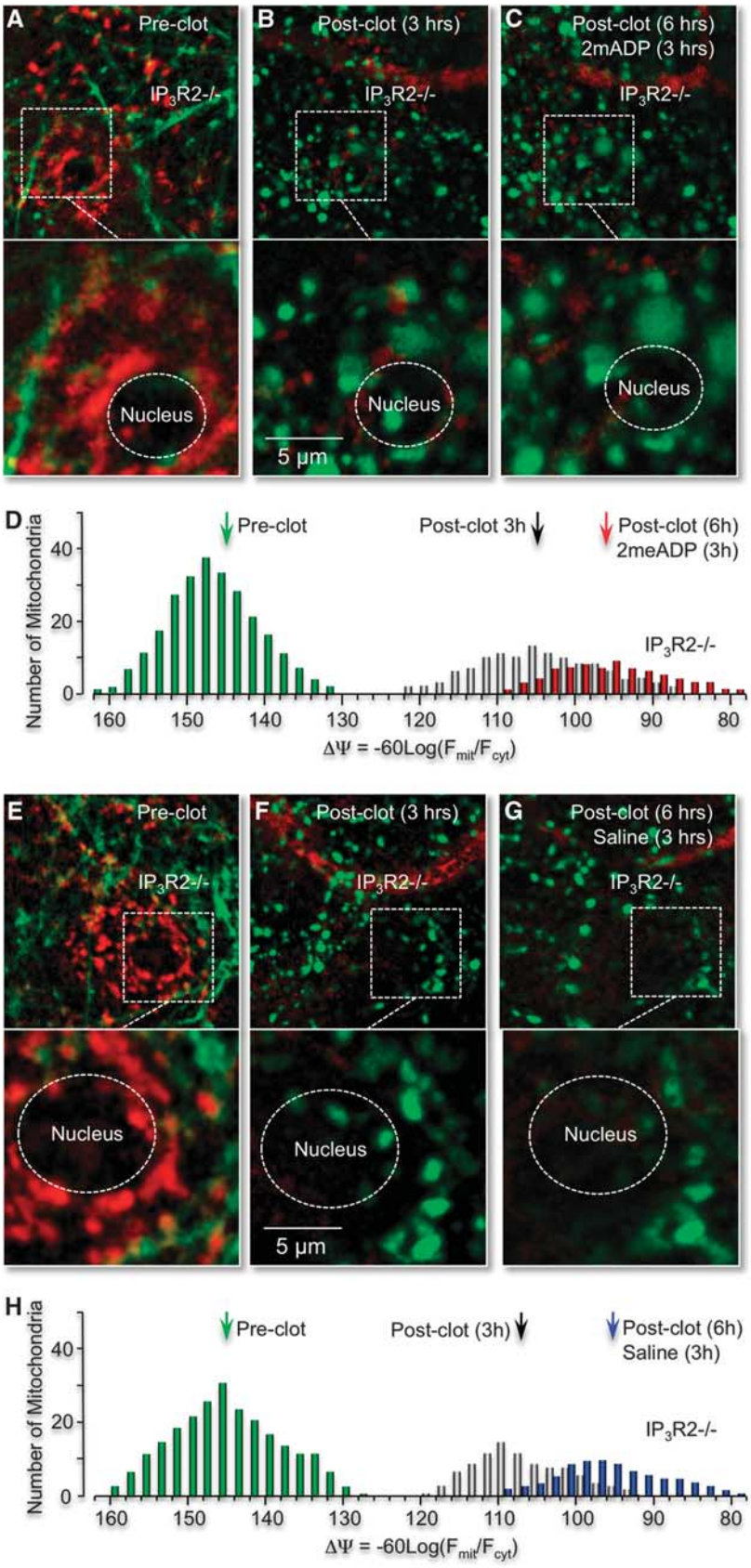

Figure 6. For caption refer page 607.

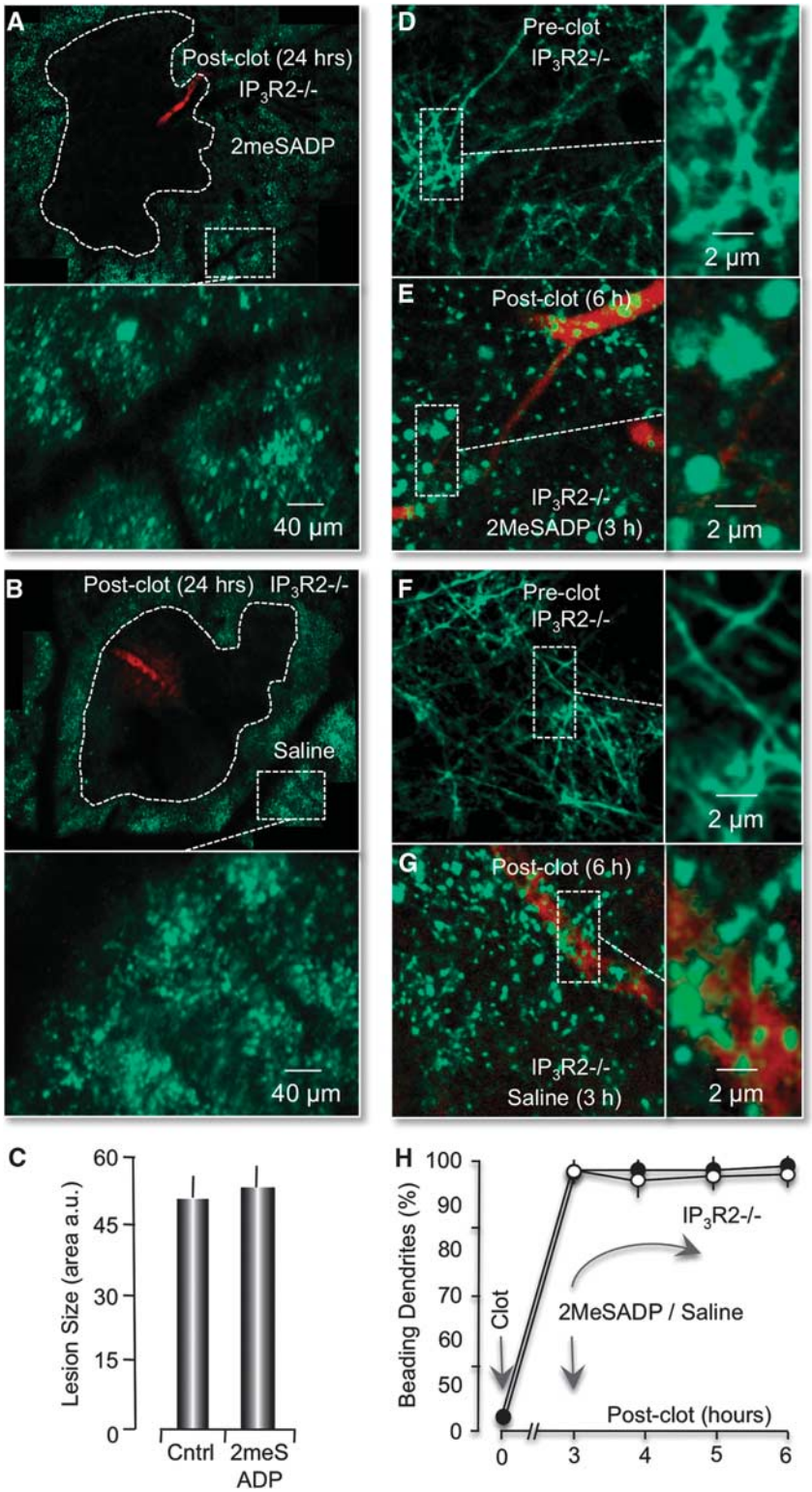

Figure 7. Photothrombotic lesions in $IP_3R2-/-$ mice are not reduced by treatment with 2MeSADP. (**A**, **B**) Montage of confocal images of dendrites (green pixels) 24 hours after an RB-induced clot (red pixels). Image acquisition and presentation are identical to Figures 1C and 1D. RB-induced neuronal lesions are traced with dotted lines. (**C**) Histogram plot of the average neuronal lesion size of four $IP_3R2-/-$ mice (RB only) and four 2MeSADP-treated $IP_3R2-/-$ mice. (**D**–**G**) $P2Y_1R$ stimulation by 2MeSADP does not reverse ischemic dendritic damage in $IP_3R2-/-$ mice. (**D**, **E**) *In vivo* confocal images of neuronal processes in $IP_3R2-/-$ x Thy1–YFP mice before (**D**) and 6 hours after photothrombosis (**E**). 2MeSADP was tail-vein injected 3 hours after photothrombosis. (**F**, **G**). Confocal images from an RB-stroked mouse, but treated with saline at 3 hours postphotothrombosis. Image acquisition and presentation are identical to Figure 2. (**H**) Plot of the percentage of dendrites that exhibit beading ($n = 4$ mice).

stimulation.[11] It is also clear that extracellular ATP concentrations are increased following ischemia,[28] which would be expected to activate purinergic receptors in astrocytes. Taken together, these data are consistent with an endogenous neuroprotective mechanism in astrocytes activated after ischemia, inhibited by disruption of either basal IP_3R signaling or mitochondrial function and mediated, at least in part, by naturally stimulated $P2Y_1Rs$.

Depolarization and repolarization of astrocyte mitochondria potentials were correlated with the extent of both dendritic beading and swelling after photothrombotic ischemia. The assignment of cortical layer I mitochondria to astrocytes was based on the distinctive size, shape and abundance of astrocytes at layer I cortex where very few neuronal nuclei exist and the size of microglia nuclei are significantly smaller than astrocytes.[17] The accuracy of assignment was suggested by either GFP labeling from GFAP–GFP mice or astrocyte-specific dye SR101. In addition, the accuracy of assigning nuclear-associated mitochondria to astrocytes was independently tested in mice with specific genetic disruptions limited to astrocytes only. Stimulation of astrocyte-specific $P2Y_1Rs$ repolarized nuclear-associated mitochondria 3 hours after photothrombosis in control mice (Figure 4). However, $P2Y_1R$ stimulation had no affect on polarization of these nuclear-associated mitochondria in transgenic mice with astrocyte-specific knockout of IP_3R signaling (IP_3R_2 knockout mice) (Figure 6). We observed that the average mitochondrial membrane potential was near -150 mV at rest and was reduced to ~ -120 mV at 3 hours, when dendritic damage was very pronounced (Figure 4). 2MeSADP treatment repolarized mitochondria to resting levels (~ -150 mV) in parallel to the partial reversal of dendritic damage (Figure 4). Consistent with our working model of astrocyte-mediated neuroprotection, postischemic treatment of IP_3R2 knockout mice with 2MeSADP did not reverse dendritic beading and swelling and did not repolarize astrocyte mitochondrial membrane potentials (Figure 6). We found no evidence that the resting mitochondrial membrane potentials in astrocytes were affected by the absence of IP_3R2 signaling (cf. Figures 6E–6H and Figures 4G–4J). However, photothrombotic lesions of IP_3R2 knockout mice appeared to result in greater depolarization with an average potential closer to ~ -110 mV at 3 hours, before treatment with 2MeSADP (Figure 6). These data also suggest that IP_3R2-dependent signaling mediates an endogenous neuroprotective mechanism in astrocytes.

An obvious requirement for mitochondrial oxidative phosphorylation after stroke is the availability of oxygen and an energy substrate. Our observations, as well as reports by others, have shown collateral vessels nearby clotted vessels continue to flow to provide oxygen and glucose, albeit at lower level than control values.[11,13,29] Moreover, the glucose metabolic rate in acute penumbral tissue is not decreased despite significant blood flow reduction, thus leading to a markedly elevated metabolism/blood flow ratio. Glycogen stores in astrocytes may also serve as a carbon source during glucose deprivation.[30] The repolarization of astrocyte mitochondria by applying 2MeSADP after single-vessel photothrombosis indicates the supply of both oxygen and energy is adequate, regardless of the source.

That a variety of GPCRs (G-protein-coupled receptors) can stimulate IP_3-mediated Ca^{2+} release in astrocytes is well documented.[31] We reported that treatment of astrocytes with membrane permeant IP_3 alone is sufficient to stimulate mitochondrial metabolism.[20] Thus, each GPCR is expected to enhance neuroprotection when activated. However, it is important to select a GPCR that is expressed only in astrocytes, for example $P2Y_1Rs$,[11,32] since IP_3-mediated increases in mitochondrial Ca^{2+} in many cell types, including neurons, opens the mitochondrial permeability transition pore causing necrosis. Astrocytes as well as muscle cells are much less sensitive to Ca^{2+}-induced necrosis, likely due to low expression levels of cyclophilin D.[33] This makes $P2Y_1Rs$ a promising target to regulate glial metabolism and improve brain damage outcome. Moreover, we found no evidence that stimulation of $P2Y_1Rs$ induced significant, Ca^{2+}-sensitive glutamate release from astrocytes, and consequently, its stimulation may not generate excitotoxic NMDA receptor-mediated inward currents in neurons.[27]

Kazuhide Inoue and coworkers[34] have reported that stimulation of $P2Y_1Rs$ enhances long-term neuroprotection by upregulating oxidoreductase genes and stimulating interleukin 6 release. They also reported long-term neurodestructive effects after $P2Y_1R$ stimulation that appeared linked to a p-RelA-mediated NF-κB pathway that modulated the transcriptional activity of cytokine/chemokine.[35] Protective versus destructive transcriptional responses of $P2Y_1R$ stimulation may be due to the different injury models utilized in these studies: permanent ischemia versus an ischemia–reperfusion. Reperfusion after ischemia leads to a significant burst of oxidative damage absent in permanently occluded blood vessels.[36] Nevertheless, our approach is distinct in that most of our experimental data were obtained acutely (nontranscriptionally) and after permanent occlusion of blood vessels. This distinction is important to emphasize with regard to our observation that $P2Y_1R$ stimulation partially reversed ischemia-induced dendritic damage, since reperfusion itself has been shown to reverse dendritic beading and swelling.[14,19]

Overall, our data suggest that the neuroprotective effects of $P2Y_1R$ stimulation are most likely due to astrocyte-specific expression even though $P2Y_1Rs$ have been reported expressed in multiple cells types, including interneurons, microglia, and endothelial cells.[37] First, we found that expression of $P2Y_1Rs$ appears higher in astrocytes compared with other cell types when immunoprobed in mouse brain slices.[32] These data do not rule out an affect of $P2Y_1R$ expression in other cell-types, but they are consistent with astrocytes being more sensitive to $P2Y_1R$ stimulation. Irrespective of $P2Y_1R$ levels in other cell types, the neuroprotective effects that we observe appear dependent on astrocyte expression. In particular, pharmacological and genetics manipulations indicate that astrocyte mitochondrial function is required for $P2Y_1R$-enhanced neuroprotection: an astrocyte-specific tricarboxylic acid cycle toxin, fluoroacetate, blocked neuroprotection and expression of a astrocyte-specific, mitochondrially targeted DNA restriction enzyme, *Eco*RI, blocked neuroprotection.[11] Furthermore, we demonstrated in this manuscript that $P2Y_1R$-enhanced neuroprotection was dependent on expression of an IP_3R2 isoform that is primarily expressed in astrocytes (Figures 6 and 7). Independently, we measured the effect of $P2Y_1R$ stimulation on vasodilation and found no significant changes, suggesting that neuroprotection was unlikely mediated by endothelial cells.[11] Finally, all of the genetic manipulations noted above blocked $P2Y_1R$-enhanced repolarization of mitochondria associated with astrocyte nuclei, as argued above. Based on these data, we suggest that P2Y1R-enhanced neuroprotection is mediated by astrocyte-specific expression.

The specific, ATP-dependent process in astrocytes that benefits neurons remains to be elucidated. Candidate processes range from an ATP-dependent production of soluble factors, such as synthesis and release of glutathione or brain-derived neurotrophic factor,[4] to an ATP-dependent restoration of ion homeostasis. Acutely, control of Na^+ and K^+ ion levels by Na^+, K^+ ATPase activity may be critical. Increased activity of this pump after ischemia would reduce the buildup of intracellular Na^+ ions and consequently, decrease cytotoxic edema, as originally suggested by our previous study.[11] Edema not only increases pressure on neurons, but restricts blood flow, further exacerbating ischemic conditions.[38] Increased Na^+, K^+ ATPase activity would also enhance the ability of astrocytes to reduce elevated extracellular K^+ after ischemia, which would inhibit the occurrence of damaging recurrent spreading depolarizations in both neurons and astrocytes.[5,39] Recurrent spreading depolarizations are known to play a critical role in the expansion of cerebral infarcts.[6,40] They

elevate metabolic stress in the penumbra primarily due to the increased energy demands required to recovery ion homeostasis. Recurrent spreading depolarizations also depolarize excitatory neurons, stimulating an excessive release of the neurotransmitter glutamate leading to excitotoxicity.[5] In general, excitotoxicity and cell death subsequent to disruption of ion homeostasis damages adjacent tissue and expand the infarct by secondary mechanisms.[2] Irrespective of the affected end process, our results suggest that stimulation of astrocyte ATP production is potentially a robust therapeutic strategy to treat brain damage, since it is not inherently dependent on protecting or affecting a single target within neurons.

DISCLOSURE/CONFLICT OF INTEREST

The authors declare no conflict of interest.

ACKNOWLEDGEMENTS

The authors thank Professor Ju Chen for generating the IP_3R2 knockout mice and Dr Ken McCarthy for his kind help with the IP_3R2 knockout mice. The author also thank Professor Robert M Byran and Professor Emeritus Linda Swisher for their critical comments and careful critique of the manuscript. Images were generated in the Core Optical Imaging Facility supported by UTHSCSA, NIH-NCI P30 CA54174 (CTRC at UTHSCSA) and NIH-NIA P01AG19316.

AUTHOR CONTRIBUTIONS

JDL and WZ formulated the hypotheses, organized and designed the studies. WZ collected the *in vivo* optical-imaging data. LTW and DMH assisted with animal housing and JW helped with *in vivo* imaging. JDL and WZ wrote and prepared the paper and figures.

REFERENCES

1 Zhao Y, Rempe DA. Targeting astrocytes for stroke therapy. *Neurotherapeutics* 2010; **7**: 439–451.
2 Nedergaard M, Dirnagl U. Role of glial cells in cerebral ischemia. *Glia* 2005; **50**: 281–286.
3 Moskowitz MA, Lo EH, Iadecola C. The science of stroke: mechanisms in search of treatments. *Neuron* 2010; **67**: 181–198.
4 Barreto G, White RE, Ouyang Y, Xu L, Giffard RG. Astrocytes: targets for neuroprotection in stroke. *Cent Nerv Syst Agent Med Chem* 2011; **11**: 164–173.
5 Strong AJ, Dardis R. Depolarisation phenomena in traumatic and ischaemic brain injury. *Adv Tech Stand Neurosurg* 2005; **30**: 3–49.
6 Woitzik J, Back T, Thome C. Flow-dependent versus spreading-like impairment of brain tissue integrity during focal cerebral ischemia and its consequences for neuroprotective strategies. *Front Biosci* 2008; **13**: 1500–1506.
7 Hertz L, Peng L, Dienel GA. Energy metabolism in astrocytes: high rate of oxidative metabolism and spatiotemporal dependence on glycolysis/glycogenolysis. *J Cereb Blood Flow Metab* 2007; **27**: 219–249.
8 Watts LT, Lechleiter JD. The impact of astrocyte mitochondrial metabolism on neuroprotection during aging. In: Parpura V, Haydon PG (eds) *Astrocytes in (patho) Physiology of the Nervous System*. Springer: Boston, MA, 2008, pp 569–590.
9 Chu X, Fu X, Zou L, Qi C, Li Z, Rao Y *et al.* Oncosis, the possible cell death pathway in astrocytes after focal cerebral ischemia. *Brain Res* 2007; **1149**: 157–164.
10 Lin DT, Wu J, Holstein D, Upadhyay G, Rourk W, Muller E *et al.* Ca^{2+} signaling, mitochondria and sensitivity to oxidative stress in aging astrocytes. *Neurobiol Aging* 2007; **28**: 99–111.
11 Zheng W, Watts LT, Holstein DM, Prajapati SI, Keller C, Grass EH *et al.* Purinergic receptor stimulation reduces cytotoxic edema and brain infarcts in mouse induced by photothrombosis by energizing glial mitochondria. *PloS one* 2010; **5**: e14401.
12 Kilkenny C, Browne WJ, Cuthill IC, Emerson M, Altman DG. Improving bioscience research reporting: the ARRIVE guidelines for reporting animal research. *PLoS Biol* 2010; **8**: e1000412.
13 Zhang S, Murphy TH. Imaging the impact of cortical microcirculation on synaptic structure and sensory-evoked hemodynamic responses in vivo. *PLoS Biol* 2007; **5**: e119.
14 Murphy TH, Li P, Betts K, Liu R. Two-photon imaging of stroke onset in vivo reveals that NMDA-receptor independent ischemic depolarization is the major cause of rapid reversible damage to dendrites and spines. *J Neurosci* 2008; **28**: 1756–1772.
15 Ding S, Fellin T, Zhu Y, Lee SY, Auberson YP, Meaney DF *et al.* Enhanced astrocytic Ca^{2+} signals contribute to neuronal excitotoxicity after status epilepticus. *J Neurosci* 2007; **27**: 10674–10684.
16 Perry SW, Norman JP, Barbieri J, Brown EB, Gelbard HA. Mitochondrial membrane potential probes and the proton gradient: a practical usage guide. *Biotechniques* 2011; **50**: 98.
17 Swenson R. Review of clinical and functional neuroscience. *Educational Review Manual in Neurology* 2006. http://www.dartmouth.edu/~rswenson/NeuroSci/index.html.
18 Thoren AE, Helps SC, Nilsson M, Sims NR. The metabolism of 14C-glucose by neurons and astrocytes in brain subregions following focal cerebral ischemia in rats. *J Neurochem* 2006; **97**: 968–978.
19 Risher WC, Ard D, Yuan J, Kirov SA. Recurrent spontaneous spreading depolarizations facilitate acute dendritic injury in the ischemic penumbra. *J Neurosci* 2010; **30**: 9859–9868.
20 Wu J, Holstein JD, Upadhyay G, Lin DT, Conway S, Muller E *et al.* Purinergic receptor-stimulated IP_3-mediated Ca^{2+} release enhances neuroprotection by increasing astrocyte mitochondrial metabolism during aging. *J Neurosci* 2007; **27**: 6510–6520.
21 Petravicz J, Fiacco TA, McCarthy KD. Loss of IP_3 receptor-dependent Ca^{2+} increases in hippocampal astrocytes does not affect baseline CA1 pyramidal neuron synaptic activity. *J Neurosci* 2008; **28**: 4967–4973.
22 Paredes RM, Etzler JC, Watts LT, Zheng W, Lechleiter JD. Chemical calcium indicators. *Methods* 2008; **46**: 143–151.
23 Territo PR, Mootha VK, French SA, Balaban RS. Ca(2+) activation of heart mitochondrial oxidative phosphorylation: role of the F(0)/F(1)-ATPase. *Am J Physiol Cell Physiol* 2000; **278**: C423–C435.
24 Duffy S, MacVicar BA. In vitro ischemia promotes calcium influx and intracellular calcium release in hippocampal astrocytes. *J Neurosci* 1996; **16**: 71–81.
25 Quesada O, Ordaz B, Morales-Mulia S, Pasantes-Morales H. Influence of Ca^{2+} on $K+$ efflux during regulatory volume decrease in cultured astrocytes. *J Neurosci Res* 1999; **57**: 350–358.
26 Ding S, Wang T, Cui W, Haydon PG. Photothrombosis ischemia stimulates a sustained astrocytic Ca^{2+} signaling in vivo. *Glia* 2009; **57**: 767–776.
27 Shigetomi E, Bowser DN, Sofroniew MV, Khakh BS. Two forms of astrocyte calcium excitability have distinct effects on NMDA receptor-mediated slow inward currents in pyramidal neurons. *J Neurosci* 2008; **28**: 6659–6663.
28 Melani A, Turchi D, Vannucchi MG, Cipriani S, Gianfriddo M, Pedata F. ATP extracellular concentrations are increased in the rat striatum during *in vivo* ischemia. *Neurochem Int* 2005; **47**: 442–448.
29 Terpolilli NA, Kim SW, Thal SC, Kataoka H, Zeisig V, Nitzsche B *et al.* Inhalation of nitric oxide prevents ischemic brain damage in experimental stroke by selective dilatation of collateral arterioles novelty and significance. *Circ Res* 2012; **110**: 727–738.
30 Wender R, Brown AM, Fern R, Swanson RA, Farrell K, Ransom BR. Astrocytic glycogen influences axon function and survival during glucose deprivation in central white matter. *J Neurosci* 2000; **20**: 6804–6810.
31 Verkhratsky A, Kettenmann H. Calcium signalling in glial cells. *Trends Neurosci* 1996; **19**: 346–352.
32 Watts LT, Sprague S, Zheng W, Garling RJ, Jimenez D, Digicaylioglu M *et al.* Purinergic 2Y1 Receptor stimulation decreases cerebral edema and reactive gliosis in a Traumatic Brain Injury Model. *J Neurotrauma* 2013; **30**: 55–66.
33 Naga KK, Sullivan PG, Geddes JW. High cyclophilin D content of synaptic mitochondria results in increased vulnerability to permeability transition. *J Neurosci* 2007; **27**: 7469–7475.
34 Fujita T, Tozaki-Saitoh H, Inoue K. P2Y1 receptor signaling enhances neuroprotection by astrocytes against oxidative stress via IL-6 release in hippocampal cultures. *Glia* 2009; **57**: 244–257.
35 Kuboyama K, Harada H, Tozaki-Saitoh H, Tsuda M, Ushijima K, Inoue K. Astrocytic P2Y(1) receptor is involved in the regulation of cytokine/chemokine transcription and cerebral damage in a rat model of cerebral ischemia. *J Cereb Blood Flow Metab* 2011; **31**: 1930–1941.
36 Zhang S, Li H, Yang SJ. Tribulosin protects rat hearts from ischemia/reperfusion injury. *Acta Pharmacol Sin* 2010; **31**: 671–678.
37 Burnstock G. Introduction to purinergic signalling in the brain. *Adv Exp Med Biol* 2013; **986**: 1–12.
38 Rosand J, Schwamm LH. Management of brain edema complicating stroke. *J Intensive Care Med* 2001; **16**: 128–141.
39 Nedergaard M. Spreading depression as a contributor to ischemic brain damage. *Adv Neurol* 1996; **71**: 75–83.
40 Dirnagl U, Iadecola C, Moskowitz MA. Pathobiology of ischaemic stroke: an integrated view. *Trends Neurosci* 1999; **22**: 391–397.

Supplementary Information accompanies the paper on the Journal of Cerebral Blood Flow & Metabolism website (http://www.nature.com/jcbfm)